Journal of Cerebral Blood Flow & Metabolism (2011) 31, 36–40

www.jcbfm.com

Brief Communication

Dynamics of regional distribution of ischemic lesions in middle cerebral artery trunk occlusion relates to collateral circulation

Bastian Cheng[1], Amir Golsari[1], Jens Fiehler[2], Michael Rosenkranz[1], Christian Gerloff[1] and Götz Thomalla[1]

[1]*Klinik und Poliklinik für Neurologie, Kopf- und Neurozentrum, Universitätsklinikum Hamburg-Eppendorf, Hamburg, Germany;* [2]*Klinik und Poliklinik für Neuroradiologische Diagnostik und Intervention, Diagnostikzentrum Universitätsklinikum Hamburg-Eppendorf, Hamburg, Germany*

We describe the regional distribution of acute perfusion, diffusion, and final infarct lesions in middle cerebral artery (MCA) trunk occlusion. A total of 31 patients with acute ischemic stroke and MCA trunk occlusion were studied by multiparametric magnetic resonance imaging. Probabilistic maps of lesion distribution were generated. The probability of initial and final infarcts was highest in the central MCA region with decreasing probability toward the periphery where the probability of the tissue at risk of infarction to be saved was highest. The probability of brain regions being involved in acute diffusion lesions and evolving into or escaping from the final infarct relates to the anatomy of arterial blood supply.
Journal of Cerebral Blood Flow & Metabolism (2011) **31,** 36–40; doi:10.1038/jcbfm.2010.185; published online 13 October 2010

Keywords: magnetic resonance imaging, diffusion weighted; magnetic resonance imaging, perfusion weighted; stroke, acute; tissue plasminogen activator

The site of cerebral vessel occlusion determines the regional pattern and temporal evolution of infarct lesions in acute ischemic stroke (Fiehler *et al*, 2005; Phan *et al*, 2005). Knowledge of these characteristics represents the basis for the interpretation of acute stroke imaging findings in clinical practice and research. Given the frequency of acute middle cerebral artery (MCA) occlusion, the number of studies that systematically characterize the regional distribution of acute ischemic lesions is surprisingly small (Phan *et al*, 2005).

We used multiparametric stroke magnetic resonance imaging (MRI) with perfusion imaging (PI) and diffusion-weighted imaging (DWI) to characterize the dynamics of regional lesion distribution in acute ischemic stroke patients with MCA main stem occlusion. To avoid potential confounding treatment effects, we only included patients treated with intravenous thrombolysis with tissue plasminogen activator (IV-tPA).

Correspondence: B Cheng, MD, Klinik und Poliklinik für Neurologie, Kopf- und Neurozentrum, Universitätsklinikum Hamburg-Eppendorf, Martinistr., 52, 20246 Hamburg, Germany.
E-mail: b.cheng@uke.uni-hamburg.de
Received 3 June 2010; revised 18 August 2010; accepted 20 September 2010; published online 13 October 2010

Subjects and methods

Sample

We retrospectively analyzed data collected within a prospective study of MRI-based treatment with IV-tPA within our center (Thomalla *et al*, 2006). Inclusion criteria for the current analysis were: (1) acute ischemic stroke; (2) stroke MRI performed within 6 hours of symptom onset; (3) MCA main stem occlusion identified by time-of-flight MR angiography (patients with additional occlusion of the anterior cerebral artery, posterior cerebral artery, or internal carotid artery were excluded); (4) treatment with IV-tPA; (5) follow-up time-of-flight MR-angiography MCA 24 hours after stroke onset; and (6) follow-up MRI 3 to 6 days after stroke. Treatment with IV-tPA was performed according to an institutional protocol up to 6 hours after symptom onset.

Magnetic Resonance Imaging Protocol and Analysis

Magnetic resonance imaging studies were performed on a 1.5-T scanner (Magnetom Symphony/Sonata; Siemens, Erlangen, Germany), using a standardized stroke MRI protocol as reported previously (Fiehler *et al*, 2005). In each patient, we defined six regions of interest: acute PI lesion, acute DWI lesion, PI/DWI mismatch, final infarct,

saved tissue at risk, and infarct growth. Acute PI lesions were determined on time-to-peak (TTP) maps, applying a threshold of a TTP delay of >4 seconds as compared with the mean TTP of the unaffected hemisphere using MR Vision (MR Vision Co., Winchester, VA, USA), according to a previously established semiautomatic procedure (Fiehler *et al*, 2005) and in accordance with a comparative PET (positron emission tomography)-MRI study, in which a TTP threshold >4 seconds best identified severe hypoperfusion corresponding to <20 mL/100 g per minute as assessed by ^{15}O-water PET (Sobesky *et al*, 2004). Acute DWI lesions and final infarct lesions were delineated on acute and follow-up $b=1{,}000$ images, and defined by a signal intensity exceeding the mean signal intensity of the unaffected hemisphere by >2 s.d. The TTP maps and follow-up images were coregistered to acute DWI using FLIRT (FMRIB's Linear Image Registration Tool) from the FSL (FMRIB Software Library, Oxford, UK) (Jenkinson *et al*, 2002). After coregistration, PI-DWI mismatch (=acute PI lesion−acute DWI lesion), saved tissue at risk (=acute PI lesion−final infarct lesion), and infarct growth (=final infarct lesion−initial DWI) were calculated. All images were transferred to standard space: first, nondiffusion-weighted images ($b=0$) from acute DWI were registered to standard Montreal Neurological Institute (MNI) space using affine transformation in FLIRT, and then the transformation matrix was applied to the lesion region-of-interest images. Images of patients with right MCA occlusion were mirrored across the y axis. Finally, lesion regions of interest were smoothed using a Gaussian filter of 4 mm full-width half-maximum to balance inaccuracies of coregistration and to correct for the lower in plane resolution of the perfusion images that had to be fitted to the echo-planar image (EPI) template. Group maps (I_g) were created calculating the mean of n images: $I_g=(I_1+I_2+I_{3\ldots}I_n)/n$ for each lesion region of interest. Regional lesion probability was evaluated by visual inspection of the probability of lesion overlap with anatomic landmarks using the integrated maps in FSL. Recanalization was assessed on follow-up time-of-flight MR angiography after 24 hours using a modified TIMI (thrombolysis in myocardial infarction) scale as suggested previously (Neumann-Haefelin *et al*, 2004) and dichotomized into recanalization (=partial or complete recanalization, TIMI 2 or 3) and no recanalization (=persistent occlusion or minimal recanalization, TIMI 0 or 1).

The study was approved by the institutional ethics committee.

Results

Patient Data

Of 57 patients fulfilling the inclusion criteria, 26 were excluded because of insufficient image quality ($n=20$), surgical treatment ($n=1$), intracranial bleeding ($n=3$), and enrolment in randomized clinical trials ($n=2$). Finally, 31 patients were included, 16 females (52%) and 15 males (48%), median age 73 (range 47 to 87) years, National Institute of Health Stroke Scale (NIHSS) on admission 16 (2 to 25), occlusion of the left MCA in $n=14$ (45%), of the right MCA in $n=17$ (55%). Intravenous thrombolysis with tissue plasminogen activator was administered within 3 hours after symptom onset in 16 patients (52%) and after 3 to 6 hours in 15 patients (48%). After 24 hours, recanalization of the MCA was shown in $n=18$ (58%), and no recanalization was detected in $n=13$ (42%).

Topography of Lesion Distribution

In the majority of patients, the acute DWI lesion involved the striatocapsular region (lesion probability 80% to 100% in the lentiform nucleus and 60% to 80% in the caudate nucleus) with decreasing probability toward the insula and centrum semiovale, completely sparing the superficial MCA territory (Figure 1). The acute PI lesion almost involved the entire MCA territory. Probability decreased toward the periphery in all directions. The PI/DWI mismatch pattern showed a similar distribution, while excluding large parts of the striatocapsular region.

Follow-up imaging showed the highest probability of final infarct in the striatocapsular region (up to 100%) and in the insula (60% to 80%), decreasing toward frontal, temporal, and parietal cortical areas. Infarct growth was most likely to be found in the striatocapsular region (20% to 60%), centrum semiovale, and central cortical and subcortical areas of the frontal and temporal lobes (20% to 40%), while sparing large parts of the superficial anterior and posterior MCA territory. Accordingly, the saved tissue at risk was identified across the entire MCA territory with the highest frequencies in superficial frontal, temporal, and parietal cortical regions (60% to 80%), completely sparing the striatocapsular region.

Comparing two subgroups of patients with successful and failed recanalization of the MCA (Figure 2), slight differences were already visible in the initial distribution of acute DWI lesions at the lentiform nucleus and pallidum, which were more likely (80% versus 60% and 50% versus 30%) to be involved in the nonrecanalization group, whereas involvement of the insular cortex was less likely (0% versus 45%). Acute PI lesion*s* did not show any obvious differences between both groups, and the PI/DWI mismatch pattern differed slightly according to the pattern of acute DWI lesions. Lesion patterns of final infarct and infarct growth were comparable in both groups, although there was a tendency of the insular region to be affected more often in the nonrecanalization group. The saved tissue at risk was identified in both groups in a similar distribution.

Discussion

In this probabilistic analysis, we describe the dynamics of the regional distribution of acute

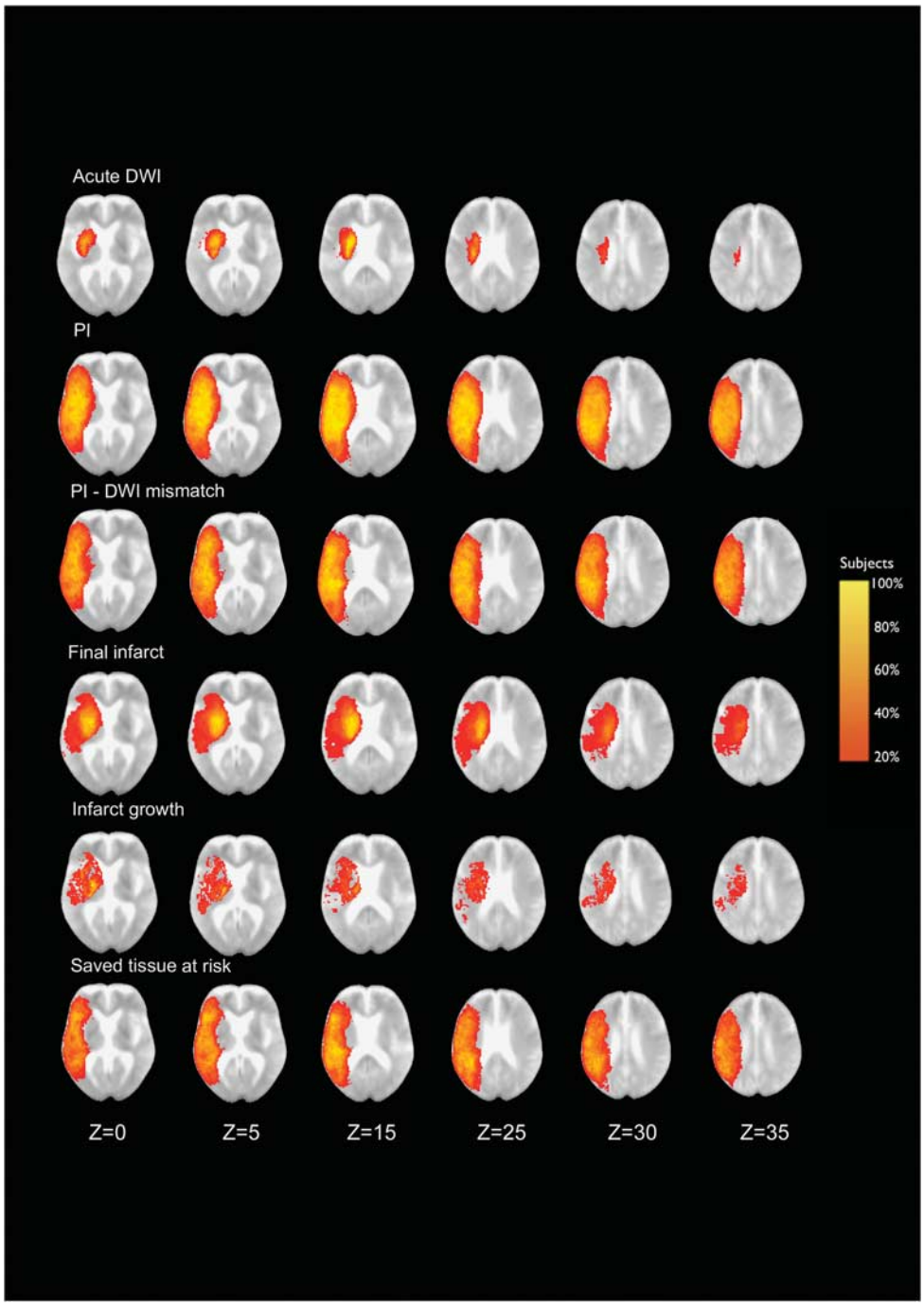

Figure 1 Shows the probabilistic distribution of the six-lesion ROI in a standard MNI space superimposed on a mean image of spatially normalized nondiffusion-weighted ($b = 0$) images of all patients ($n = 31$). *Z* coordinates are given in millimeters. ROI, region of interest.

ischemic lesions in a homogenous sample of patients with MCA main stem occlusion. Thereby, the probability of specific brain regions being involved in acute diffusion or perfusion lesion and evolving into or escaping from the final infarct was found to relate to the anatomy of arterial blood supply. In particular, the pattern of initial perfusion lesion virtually reflects the territory supplied by the MCA with a certain amount of interindividual variability. In contrast, areas with restricted diffusion were confined to the striatocapsular region, which is supplied by small-diameter penetrating arteries behaving as end arteries (Liebeskind, 2003). Consecutively, final infarct lesions enclosed most parts of the striatocapsular region in almost 100% of patients, which is in line with previous studies, reporting the striatocapsular region to be affected by infarction resulting from MCA occlusion with high

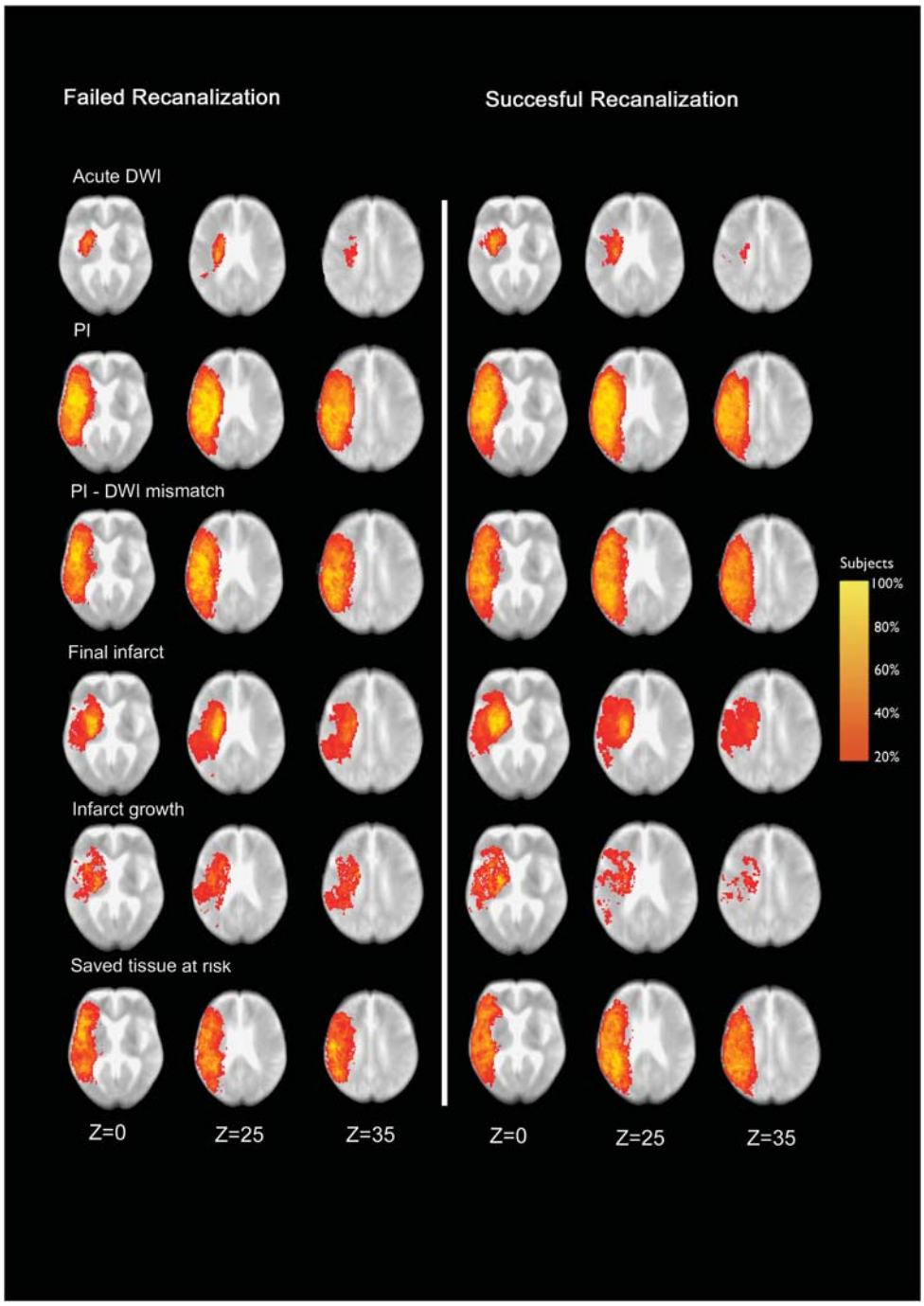

Figure 2 Shows the probabilistic distribution of the six-lesion ROI in a standard MNI space superimposed on a mean image of spatially normalized nondiffusion-weighted ($b = 0$) images of patients with failed (left side, $n = 13$) and successful (right side, $n = 18$) recanalization. *Z* coordinates are given in millimeters. ROI, region of interest.

probability (Caviness *et al*, 2002; Phan *et al*, 2005). A decreased lesion frequency was found toward the border zone areas, which are additionally supplied by collateral flow by anastomoses with the anterior and posterior cerebral arteries (Christensen *et al*, 2008; Liebeskind, 2003). Superficial compartments of the MCA territory, which are also reached by collateral blood flow through leptomeningeal arteries, were also spared from infarction in most patients, although involved in the acute perfusion lesion.

Previous studies have used regional information on ischemic lesion distribution to generate maps of topographic lesion distribution (Phan *et al*, 2009), to correlate infarct location with stroke severity (Menezes *et al*, 2007), and to generate statistical outcome parameters on a voxelwise analysis (Wu *et al*, 2006). Our study exceeds previous digital maps

by characterizing the dynamics of lesion evolution from the first hours of stroke to the early subacute stage, incorporating information on tissue characteristics from multiparametric MRI, including acute perfusion and diffusion maps. We were able to show that the probability of the tissue at risk proceeding to infarction was highest in central parts of the MCA territory (striatocapsular, insular, opercular region, and central and precentral cortices).

The extent to which the final diffusion lesion overlaps within the MCA territory has been shown to vary depending on the time point of proximal MCA recanalization after ischemic infarction. Larger areas were affected in failed recanalization assessed <24 hours (Seitz *et al*, 2009) and delayed (>6 hours) or failed recanalization assessed >24 hours in comparison with early recanalization $\leqslant 6$ hours after stroke onset (Humpich *et al*, 2006). In our study, no obvious differences in the extent of final infarct lesions were detected comparing patients with and without successful recanalization. However, this might be explained by the time point of assessment of recanalization, which was not before 24 hours after stroke onset in our study. A number of patients with patent MCA after 24 hours might have experienced late nonnutritional reperfusion, i.e., at a time when tissue damages were already irreversible.

There are limitations to our study. Inclusion criteria might have led to a selection bias excluding very severely affected patients precluding follow-up MRI. We did not analyze gray matter and white matter separately; thus, we cannot draw any conclusions on possible differences in vulnerability to acute ischemia between gray matter and white matter, which have been reported previously (Koga *et al*, 2005).

To summarize, the regional distribution of acute diffusion and perfusion lesions and final infarct in acute MCA main stem occlusion relates to the anatomy of arterial supply. We provide voxel-based probabilistic maps of tissue at risk of proceeding to infarction or being saved from using multiparametric MRI as applied in clinical imaging in acute stroke. In terms of clinical implications, knowledge about the dynamics of the regional distribution of ischemic lesions and tissue vulnerability depending on collateral supply may help guiding treatment decisions in acute ischemic stroke.

Disclosure/conflict of interest

The authors declare no conflict of interest.

References

Caviness VS, Makris N, Montinaro E, Sahin NT, Bates JF, Schwamm L, Caplan D, Kennedy DN (2002) Anatomy of stroke, part I: an MRI-based topographic and volumetric system of analysis. *Stroke* 33:2549–56

Christensen S, Calamante F, Hjort N, Wu O, Blankholm AD, Desmond P, Davis S, Ostergaard L (2008) Inferring origin of vascular supply from tracer arrival timing patterns using bolus tracking MRI. *J Magn Reson Imaging* 27:1371–81

Fiehler J, Knudsen K, Thomalla G, Goebell E, Rosenkranz M, Weiller C, Rother J, Zeumer H, Kucinski T (2005) Vascular occlusion sites determine differences in lesion growth from early apparent diffusion coefficient lesion to final infarct. *AJNR Am J Neuroradiol* 26:1056–61

Humpich M, Singer OC, du Mesnil de Rochemont R, Foerch C, Lanfermann H, Neumann-Haefelin T (2006) Effect of early and delayed recanalization on infarct pattern in proximal middle cerebral artery occlusion. *Cerebrovasc Dis* 22:51–6

Jenkinson M, Bannister P, Brady M, Smith S (2002) Improved optimization for the robust and accurate linear registration and motion correction of brain images. *Neuroimage* 17:825–41

Koga M, Reutens DC, Wright P, Phan T, Markus R, Pedreira B, Fitt G, Lim I, Donnan GA (2005) The existence and evolution of diffusion-perfusion mismatched tissue in white and gray matter after acute stroke. *Stroke* 36:2132–7

Liebeskind DS (2003) Collateral circulation. *Stroke* 34:2279–84

Menezes NM, Ay H, Wang Zhu M, Lopez CJ, Singhal AB, Karonen JO, Aronen HJ, Liu Y, Nuutinen J, Koroshetz WJ, Sorensen AG (2007) The real estate factor: quantifying the impact of infarct location on stroke severity. *Stroke* 38:194–7

Neumann-Haefelin T, du Mesnil de Rochemont R, Fiebach JB, Gass A, Nolte C, Kucinski T, Rother J, Siebler M, Singer OC, Szabo K, Villringer A, Schellinger PD (2004) Effect of incomplete (spontaneous and postthrombolytic) recanalization after middle cerebral artery occlusion: A magnetic resonance imaging study. *Stroke* 35:109–14

Phan TG, Donnan GA, Wright PM, Reutens DC (2005) A digital map of middle cerebral artery infarcts associated with middle cerebral artery trunk and branch occlusion. *Stroke* 36:986–91

Phan TG, Fong AC, Donnan GA, Srikanth V, Reutens DC (2009) Digital probabilistic atlas of the border region between the middle and posterior cerebral arteries. *Cerebrovasc Dis* 27:529–36

Seitz RJ, Sondermann V, Wittsack HJ, Siebler M (2009) Lesion patterns in successful and failed thrombolysis in middle cerebral artery stroke. *Neuroradiology* 51:865–71

Sobesky J, Zaro Weber O, Lehnhardt FG, Hesselmann V, Thiel A, Dohmen C, Jacobs A, Neveling M, Heiss WD (2004) Which time-to-peak threshold best identifies penumbral flow? A comparison of perfusion-weighted magnetic resonance imaging and positron emission tomography in acute ischemic stroke. *Stroke* 35:2843–7

Thomalla G, Schwark C, Sobesky J, Bluhmki E, Fiebach JB, Fiehler J, Zaro Weber O, Kucinski T, Juettler E, Ringleb PA, Zeumer H, Weiller C, Hacke W, Schellinger PD, Rother J (2006) Outcome and symptomatic bleeding complications of intravenous thrombolysis within 6 hours in MRI-selected stroke patients: comparison of a German multicenter study with the pooled data of ATLANTIS, ECASS, and NINDS tPA trials. *Stroke* 37:852–8

Wu O, Christensen S, Hjort N, Dijkhuizen RM, Kucinski T, Fiehler J, Thomalla G, Rother J, Ostergaard L (2006) Characterizing physiological heterogeneity of infarction risk in acute human ischaemic stroke using MRI. *Brain* 129:2384–93